Uncertainty Considerations for Describing Complex Reaction Systems

S. Balakrishnan and P. Georgopoulos
Dept. of Chemical Engineering, Rutgers University, Piscataway, NJ 08854 and Environmental and Occupational Health Sciences Institute, UMDNJ - R.W. Johnson Medical School and Rutgers University, Piscataway, NJ 08854

I. Banerjee and M. Ierapetritou
Dept. of Chemical Engineering, Rutgers University, Piscataway, NJ 08854

Models that accurately describe chemical processes are often intricate involving numerous reacting species and reaction steps. For complex reaction mechanisms, output-species concentration profiles can change dramatically based on the set of values chosen for inputs if they are nondeterministic. A systematic uncertainty analysis can provide insight into the level of confidence of model estimates and aid mechanism reduction. Response surface methods and variants, thereof, require much fewer simulations for the adequate estimation of system uncertainty characteristics. This article focuses on reaction rate constant uncertainty using the stochastic response surface method (SRSM), whereby, uncertain outputs are expressed in terms of a polynomial chaos expansion of Hermite polynomials and engenders such useful properties as the mean and variance and computation of sensitivity information. SRSM determines the uncertainty propagation characteristics very accurately, while using an order-of-magnitude fewer model simulations than traditional Monte Carlo techniques. Since uncertainty in kinetic rate parameters largely affects the reduction of kinetic models, a framework of analysis is also developed for mechanism reduction considering uncertainty using sensitivity information from SRSM to create good initial sets of reactions for the efficient solution of a multiperiod optimization problem. Two case studies — an isothermal supercritical wet oxidation process and a nonisothermal H_2/CO/air combustion process — elucidate the application of this framework of analysis to complex kinetic mechanisms and illustrate the possible ease of computational burden associated with mechanism reduction under uncertainty.

Introduction

Accurate models that correctly describe chemical processes are often intricate and involve a large number of reacting species and reaction steps; examples include combustion processes and atmospheric chemistry problems. Since the source of reaction rate constant parameter data is usually experimental, when dealing with complex kinetic reaction models, a certain level of uncertainty is inherent in the system. A systematic uncertainty analysis of the system can provide insight into the level of confidence of model estimates and help identify key sources of uncertainty. Conventional techniques of uncertainty propagation, however, typically require a large number of model runs that sample various combinations of the inputs, resulting in heavy computational demand (such as Monte Carlo, Latin hypercube methods). Response surface methods and variants, thereof, try to address this problem by reducing the number of simulations required for adequate estimation of uncertainty propagation.

Stochastic response surface method [SRSM, (Isukapalli, 1990)] is one such technique that uses computationally efficient instantiations of the random variables responsible for uncertainty in order to capture uncertainty effects. Based primarily on classic response surface methods and deterministic equivalent modeling [DEMM, (Tatang, 1995)], SRSM expan-

---

Correspondence concerning this article should be addressed to M. Ierapetritou.

sions express random outputs in terms of the polynomial chaos expansion (Ghanem and Spanos, 1991) of Hermite polynomials and the implementation utilizes an efficient collocation scheme combined with regression in order to determine the coefficients of the expansion. This polynomial form then engenders many useful properties, including straightforward determination of statistics like the mean and variance and computation of sensitivity information.

The complexity and intricacy of detailed kinetic models implies a heavy computational burden associated with the solution of such systems. A useful approach to overcome this computational demand associated with the inclusion of all reaction steps is kinetic mechanism reduction. Of the techniques that exist for model reduction, the approach we adopt in this work follows that developed by Androulakis (Androulakis, 2000), which is to set up and solve an optimization problem that aims to find a subset of reactions and species of the full model that produce similar (within a user-specified tolerance) concentration/temperature profiles for certain output species (tagged species).

The presence of uncertainty in model parameters complicates reaction mechanism reduction in this formulation because the reduction strategy restricts prediction error (full vs. reduced mechanism tagged species profiles) to lie below a specified limit and the set of values chosen for the uncertain inputs can dramatically change output species concentration profiles.

In this work, we focus on complex kinetic mechanism uncertainty analysis and mechanism reduction, with the aim of providing an efficient, accurate, and systematic framework of analysis that effectively deals with reaction rate constant uncertainty. SRSM is the chosen method of uncertainty analysis and is shown to be very accurate in determining the uncertainty propagation characteristics while using orders-of-magnitude fewer model simulations than traditional Monte Carlo techniques. In addition, a mechanism reduction strategy is outlined wherein very good initial sets of reactions for optimization problems are obtained via uncertainty/sensitivity analysis utilizing SRSM.

Two case studies are analyzed, an isothermal supercritical wet oxidation process (Phenix et al., 1998) and a nonisothermal H_2/CO/air combustion process (Li and Rabitz, 1997), that elucidate the application of this framework of analysis, and the results point to a substantial decrease in the computational burden associated with mechanism reduction.

Uncertainty Analysis

The presence of uncertainty often complicates the mechanistic modeling of physical systems. Uncertainty arises in such modeling efforts through various channels: natural or irreducible uncertainty, wherein the physical system being modeled itself is inherently uncertain (Brownian motion, and so on); model uncertainty, which is engendered through many correlated factors such as the model structure and approximations used, extrapolations, and model boundaries and model resolution; parametric and data uncertainty, which include experimental and data measurement errors, and imprecise device calibration biases.

The purpose of systematic uncertainty analysis is to provide insight into the level of confidence in model estimates, identify key sources of uncertainty, and quantify the degree of confidence in the existing data and models. The first step in such an analysis requires the selection of an approach for the representation of uncertainty. Of the number of techniques available (set theory, interval mathematics, fuzzy set theory, and so on) probabilistic and statistical representation of uncertainty has gained extremely wide acceptance and is the approach adopted in this study.

Of commonly employed sampling-based probabilistic/statistical methods, the Monte Carlo technique is one of the most popular. Given input uncertainty distributions (frequency or probability density data), these methods involve a repeated generation of pseudorandom instantiations of inputs followed by an application of the model to these instantiations to yield a set of model responses. These model outputs are then further analyzed statistically.

A well-known disadvantage of sampling-based techniques such as Monte Carlo is the large number of model simulations typically required to achieve acceptable levels of confidence about model output uncertainty characterization. Also, although the analysis is extremely simple to apply, the results generated have very limited use outside of uncertainty characterization. These issues underly the use of alternative, efficient, methods of uncertainty propagation such as the SRSM.

Stochastic Response Surface Method

The SRSM (Isukapalli, 1999) is an extension of the classic deterministic RSM and the DEMM. The motivation underlying the use of SRSM is to reduce the number of model simulations required for adequate estimation of uncertainty, as compared to conventional methods. This is accomplished by approximating both inputs and outputs of the uncertain system through series expansions of standard random variables; the series expansions of the outputs contain unknown coefficients that can be calculated from the results of a limited number of model simulations. Example applications where the method has been successfully applied to a variety of cases can be found in Isukapalli (Isukapalli, 1999; Isukapalli et al., 2000, 1998).

Evaluating an SRSM expansion consists of the following steps (Figure 1): (1) input uncertainties are expressed in terms of a set of standard random variables (srvs); (2) a functional form is assumed for selected outputs or output metrics; and (3) the parameters of the functional approximation are determined.

The srvs are selected from a set of independent, identically distributed (iid) normal random variables, $\{\xi_i\}_{i=1}^{n}$, where n is the number of independent inputs, and each ξ_i has zero mean and unit variance. When the input random variables are independent, the uncertainty in the ith model input X_i, is expressed directly as a function of the ith srv, ξ_i; that is, a transformation of X_i to ξ_i is employed. Such transformations are useful in the standardized representation of the random inputs, each of which could have very different distribution properties. Table 1 presents a list of transformations for some probability distributions commonly employed in transport-transformation modeling (note that currently, multimodal distributions cannot be handled by SRSM). In cases where the random inputs are correlated (and the interdependence of the variables described by a correlation matrix), a

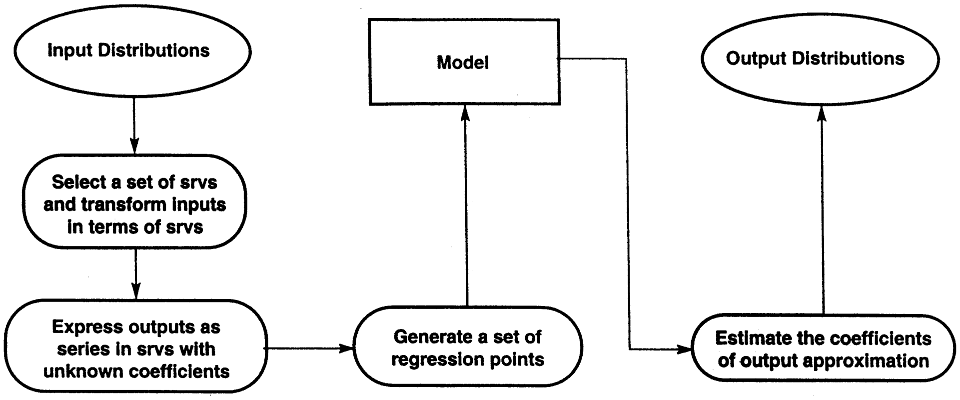

Figure 1. Steps involved in generating an SRSM expansion.

transformation process can be applied to the inputs as outlined in Isukapalli (1999).

The next step involved in implementing SRSM is expressing the series expansion of normal random variables in terms of Hermite polynomials, the "polynomial chaos expansion" (Ghanem and Spanos, 1991). When normal random variables are used as srvs, an output can be approximated by a polynomial chaos expansion on the set $\{\xi_i\}_{i=1}^n$, given by

$$y = a_0 + \sum_{i_1=1}^{n} a_{i_1}\Gamma_1(\xi_{i_1}) + \sum_{i_1=1}^{n}\sum_{i_2=1}^{i_1} a_{i_1 i_2}\Gamma_2(\xi_{i_1},\xi_{i_2}) + \sum_{i_1=1}^{n}\sum_{i_2=1}^{i_1}\sum_{i_3=1}^{i_2} a_{i_1 i_2 i_3}\Gamma_3(\xi_{i_1},\xi_{i_2},\xi_{i_3}) + \cdots \tag{1}$$

where y is any output metric (or random output) of the model, the $a_{i_1\ldots}$'s are deterministic constants to be evaluated, and the $\Gamma_p(\xi_{i_1},\ldots,\xi_{i_p})$ are multidimensional Hermite polynomials of degree p, given by

$$\Gamma_p(\xi_{i_1},\ldots,\xi_{i_p}) = (-1)^p e^{1/2\boldsymbol{\xi}^T\boldsymbol{\xi}} \frac{\partial^p}{\partial\xi_{i_1}\cdots\partial\xi_{i_p}} e^{-1/2\boldsymbol{\xi}^T\boldsymbol{\xi}} \tag{2}$$

where $\boldsymbol{\xi}$ is the vector of p iid normal random variables, $\{\xi_{i_k}\}_{k=1}^p$, that are used to represent input uncertainty. Hermite polynomials on $\{\xi_i\}_{i=1}^n$ are random variables, since they are functions of the random variables $\{\xi_i\}_{i=1}^n$. Furthermore, the Hermite polynomials defined on $\{\xi_i\}_{i=1}^n$ are orthogonal with respect to an inner product defined as the expectation of the product of two random variables (Ghanem and Spanos, 1991). Thus

$$E[\Gamma_p\Gamma_q] = 0 \quad \text{iff} \quad \Gamma_p \neq \Gamma_q$$

It is known that the set of multidimensional Hermite polynomials form an orthogonal basis for the space of square-integrable pdfs, and that the polynomial chaos expansion is convergent in the mean-square sense (Ghanem and Spanos, 1991).

For example, an uncertain model output, U, can be expressed as first-, second-, and third-order Hermite polynomial approximations, U_1, U_2, and U_3 as follows

$$U_1 = a_{0,1} + \sum_{i=1}^{n} a_{i,1}\xi_i \tag{3}$$

$$U_2 = a_{0,2} + \sum_{i=1}^{n} a_{i,2}\xi_i + \sum_{i=1}^{n} a_{ii,2}(\xi_i^2 - 1) + \sum_{i=1}^{n-1}\sum_{j>i}^{n} a_{ij,2}\xi_i\xi_j \tag{4}$$

$$U_3 = a_{0,3} + \sum_{i=1}^{n} a_{i,3}\xi_i + \sum_{i=1}^{n} a_{ii,3}(\xi_i^2 - 1) + \sum_{i=1}^{n} a_{iii,3}(\xi_i^3 - 3\xi_i) + \sum_{i=1}^{n-1}\sum_{j>i}^{n} a_{ij,3}\xi_i\xi_j + \sum_{i=1}^{n}\sum_{j=1}^{n} a_{ijj,3}(\xi_i\xi_j^2 - \xi_i) + \sum_{i=1}^{n-2}\sum_{j>i}^{n-1}\sum_{k>j}^{n} a_{ijk,3}\xi_i\xi_j\xi_k \tag{5}$$

where n is the number of srvs used to represent the uncertainty in the model inputs, and the coefficients to be estimated are $a_{i,m}$, $a_{ij,m}$, $a_{ijj,m}$, and $a_{ijk,m}$ (where m represents the order of polynomial expansion).

From the preceding equations, it can be seen that the number of unknowns to be determined for the first-, second-, and third-order polynomial chaos expansions of dimension n, denoted by N_1, N_2, and N_3, respectively, are

$$N_1 = 1 + n \tag{6}$$

Table 1. Common Univariate Distributions as Functionals of Standard Random Variables

Distribution Type	Transformation*
Uniform (a,b)	$a + (b-a)\left[\frac{1}{2} + \frac{1}{2}(\xi/\sqrt{2})\right]$
Normal (μ,σ)	$\mu + \sigma\xi$
Lognormal (μ,σ)	$\exp(\mu + \sigma\xi)$
Gamma (a,b)	$ab\left[\xi\sqrt{\frac{1}{9a}} + 1 - \frac{1}{9a}\right]^3$
Exponential (λ)	$-\frac{1}{\lambda}\log\left[\frac{1}{2} + \frac{1}{2}(\xi/\sqrt{2})\right]$
Weibull (a)	$y^{1/a}$
Extreme Value	$-\log(y)$

*ξ is normal (0,1) and y is exponential (1) distributed.

$$N_2 = 1 + 2n + \frac{n(n-1)}{2} \quad (7)$$

$$N_3 = 1 + 3n + \frac{3n(n-1)}{2} + \frac{n(n-1)(n-2)}{6} \quad (8)$$

Guided by computational constraints and accuracy requirements, the appropriate order of expansion (m) should be chosen. Because the procedure for this choice (as we advise) involves the outputs of the polynomial chaos expansion, we defer the guidelines for this choice until the end of this section (after the process of estimating the SRSM polynomial coefficients has been explained).

The final step in the SRSM implementation is to determine these coefficients of the polynomial chaos expansion (SRSM expansion), which is done using an extension to collocation methods based on a combination of regression and an improved input sampling scheme.

In collocation methods, the estimates of model outputs are exact at a set of selected collocation points, thus, making the residual at those points equal to zero. The unknown coefficients are estimated by equating model outputs and the corresponding polynomial chaos expansion at a set of collocation points in the parameter space; the number of collocation points should be equal to the number of unknown coefficients to be found. Thus, for each output metric, a set of linear equations results with the coefficients as the unknowns; these equations can be readily solved using standard linear solvers.

The improved sampling scheme called the efficient collocation method [ECM; (Isukapalli, 1999)] selects points based on a modification of the standard orthogonal collocation method of Tatang (Tatang, 1995; Villadsen and Michelsen, 1978). The points are selected so that each standard normal random variable, ξ_i, takes the values of either zero or one of the roots of the higher-order Hermite-polynomial. A simple heuristic technique is used to select the required number of points from the large number of potential candidates: for each term of the series expansion, a "corresponding" collocation point is selected. For example, the collocation point corresponding to the constant is the origin; that is, all the standard normal variables (ξ's) are set to value zero. For terms involving only one variable, the collocation points are selected by setting all other ξ's to zero value, and by letting the corresponding variable take values as the roots of the higher-order Hermite polynomial. For terms involving two or more random variables, the values of the corresponding variables are set to the values of the roots of the higher-order polynomial, and so on. If more points "corresponding" to a set of terms are available than are needed, the points that are closer to the origin are preferred, as they fall in regions of higher probability. Furthermore, when there is still an unresolved choice, the collocation points are selected such that the overall distribution of the collocation points is more symmetric with respect to the origin. If still more points are available, the collocation point is selected randomly.

After the set of sample points is selected in the same manner as the ECM method, regression is employed to obtain more robust estimates. The number of sample points selected is higher than the number of unknown coefficients to be estimated; selecting a number of points equaling approximately twice the number of coefficients is recommended for obtaining robust estimates, and is the approach used here. The model outputs at the selected sample points are equated with the estimates from the series approximation, resulting in a set of linear equations with more equations than unknowns. This system of equations is then solved using the single-value decomposition method.

The advantage of this method is that the behavior of the model is captured reasonably well at points corresponding to regions of high probability. Thus, the pdfs of the output metrics are likely to be approximated better than by a random choice of collocation points, while following a technique similar to the "orthogonal collocation" approach. Though slightly more computationally expensive than exact collocation, this method proves to be a more robust means of estimation of coefficients of the functional approximation (Isukapalli, 1999).

Regarding the issue of selecting the appropriate order of SRSM polynomial expansion, theoretically, the choice of order (m) of expansion should be one that minimizes some sort of discrepancy measure between the actual output (U^f) and the SRSM polynomial approximation (U_m^{srsm}), for example, the mean squared error (MSE), $MSE = E[(U^f - U_m^{srsm})^2]$. Currently, there is no way to bound or estimate this quantity before choosing the order of polynomial expansion. However, Monte-Carlo-type simulations can provide insight into the magnitude of the estimated MSE. The estimated MSE together with the comparison of estimates of the probability densities obtained for outputs approximated provide for fairly easily implemented measures that can be used to guide the practitioner to an adequate choice of order of approximation. A heuristic method that reflects both accuracy needs and computational constraints was proposed by Isukapalli (1999), who advised that the lower of two successive orders of expansion be picked (such as second and third order), for which the probability density functions as estimated by the expansions are sufficiently similar. Practically, for very large and complex systems, polynomial chaos expansions with an order higher than first and second order will prove difficult to obtain. However, this is not an extreme shortcoming, since the mean square convergence has been shown in a number of applications (Isukapalli, 1999; Isukapalli et al., 2000, 1998), where SRSM expansions up to the second order have been shown to capture the uncertainty characteristics of fairly complex outputs accurately.

Kinetic Mechanism Reduction

Deterministic mechanism reduction

The kinetic mechanism reduction strategy adopted in this work follows the approach of Androulakis (Androulakis, 2000), which also provides an excellent review of reduction techniques. The primary goal is to determine reactions and species that can be omitted from the mechanism without causing the predictions of the species profiles of the reduced mechanism to deviate from the full mechanism by more than a user-specified tolerance (in a root-mean-square sense). The basic idea of this approach is to solve a dynamic MINLP problem based on integer variables (representing the inclusion or exclusion of species and reactions) using a branch-and-bound solution procedure.

The problem is formulated as follows

$$\min_{\lambda} \Phi = \sum_{i=1}^{N_R} \lambda_i \tag{9}$$

subject to

$$\chi(\boldsymbol{\lambda}) \leq \epsilon \tag{10}$$

where the discrepancy function χ (which is the measure of error incurred in dropping reactions from the mechanism), is evaluated based on the average sum of the squared time-dependent residual error between the full and reduced mechanism as:

$$\chi(\boldsymbol{\lambda}) = \sum_{j=1}^{M} \int_{t_o}^{t_f} \left[\frac{u_j^f(t) - u_j^r(t)}{u_j^f(t)} \right]^2 dt \tag{11}$$

Here u represents the value of a matched quantity (temperature, species concentration, and so on) and superscripts f and r denote full and reduced, respectively. The λ_i are binary variables representing the inclusion or exclusion of reaction i in the reduced mechanism. The actual kinetic model is set up as the solution of the material and energy balances

$$\frac{dy_k}{dt} = \frac{R_k M_k}{\rho} \qquad k = 1, 2, \ldots, N_S \tag{12}$$

$$\frac{dT}{dt} = \sum_{k=1}^{N_S} \frac{R_k M_k h_k}{\rho \overline{c_p}} \tag{13}$$

where ρ and $\overline{c_p}$ are the mixture density and specific heat at constant pressure; M_k and R_k are the molecular weight and net rate of production of species k, respectively; N_S is the number of species in the mechanism; and R_k is further determined through the expression

$$R_k = \sum_{i=1}^{N_R} \lambda_i \left(\nu_{ki}^r - \nu_{ki}^f \right) q_i \tag{14}$$

where

$$q_i = k_{f,i} \prod_{k=1}^{N_S} c_k^{\nu_{ki}^f} - k_{r,i} \prod_{k=1}^{N_S} c_k^{\nu_{ki}^r} \tag{15}$$

In the preceding expressions, q_i represents the individual intrinsic rates of reaction, with k_i being the reaction rate constant values, ν_{ki} the stoichiometric coefficients, c_k the molar concentrations, and N_R is the number of reactions in the mechanism. The specific reaction rate constant value ($k_{f,i}$) is given by the Arrhenius Law

$$k_{f,i} = A_i e^{-E_i/RT} T^{b_i} \tag{16}$$

where A_i, E_i, and b_i are the preexponential factor, the activation energy, and the temperature exponent of reaction i, respectively, and R is the gas constant. It is assumed the reactor model is plug flow (PFR), and thus requires the simultaneous integration of

$$\frac{dz}{dt} = \frac{\rho_0 u_0}{\rho} \tag{17}$$

where $\rho_0 u_0$ is the mass velocity at the entrance of the PFR.

Local sensitivity analysis (which we will, henceforth, refer to as pseudosensitivity) largely figures in this solution scheme in an attempt to reduce the size of the problem by providing a set of important reactions via preprocessing. Note that the formalism as previously set up requires a deterministic or fixed set of conditions in order to be applicable. Although a variety of reaction networks have been analyzed using this procedure, the combinatorial nature of the problem quite easily leads to large-scale problems becoming extremely expensive computationally.

Mechanism reduction considering uncertainty

Kinetic mechanism reduction gets further complicated if the parameters involved are uncertain quantities, as is commonly the case given that the reaction rate constants are determined from experimental data. The integer programming approach outlined earlier is limited to being performed at a singular set of conditions (that is, on a deterministic set of inputs, which is typically chosen to be the nominal set of conditions). In order to ascertain the effects of uncertain parameters on the mechanism reduction, a multiperiod programming approach can be used (Halemane and Grossmann, 1983). Sirdeshpande et al. (2001) used this approach in order to investigate the effects of probabilistic variability of initial conditions on the reduction scheme.

The idea behind the multiperiod approach, as applied to the case of uncertain kinetic mechanism parameters, is the following: beginning with an initial set of reactions and the rate constant values at nominal conditions, a reduced mechanism is generated (akin to a nominal reduction). Another optimization problem is then set up to find a scenario (the values of the reaction rate constants lying within their bounds) that maximizes the discrepancy given this reduced mechanism. If this discrepancy lies within the tolerance defined, the reduced mechanism at this stage is the final solution. If the discrepancy is more than acceptable, however, the scenario is then included as a constraint to the mechanism reduction itself and another (larger) reduced mechanism obtained. This process is then iterated until a final solution is obtained.

One can easily see how, at the end of this analysis, a mechanism that takes into account the uncertainty in the reaction rate constant values results, as the final reduced mechanism that is obtained from this procedure is generated to satisfy the specified tolerance criterion even for the maximum discrepancy scenario (set of rate constant values for which the error is the worst possible). One must keep in mind, however, the underlying assumption following this approach is that the mechanism is adequate for the entire range of operability (input parameter space).

Mathematically, the problem is set up as proposed by Halemane and Grossmann (1983). A population of Np vectors of uncertain parameters is generated and the MINLP problem solved with Np constraints as

$$\min_{\lambda} \Phi = \sum_{i=1}^{N_R} \lambda_i \tag{18}$$

subject to

$$\chi_k(\lambda, \theta^k) \leq \epsilon, \qquad k = 1, 2, \ldots, Np \tag{19}$$

where θ^k is the set of rate constants corresponding to a single scenario. In the first iteration, the flexibility of the reduced mechanism at nominal conditions is checked by solving the following NLP

$$\max_{\theta^{Np}} \chi \tag{20}$$

subject to

$$k_{f,i}^{LB} \leq k_{f,i} \leq k_{f,i}^{UB}, \qquad i = 1, 2, \ldots N_R. \tag{21}$$

The upper and lower bounds on the reaction rate constants are computed through the uncertainty factors as $k_{f,i}^{LB} = k_{f,i}^{\text{nom}}/UF_i$ and $k_{f,i}^{UB} = k_{f,i}^{\text{nom}} * UF_i$, where $k_{f,i}^{\text{nom}}$ represents the nominal value of the rate constant. Finding a value of $\chi > \epsilon$ indicates that the mechanism does not have the desired flexibility and the optimal θ^k values resulting from the solution of the NLP (Eq. 20) are introduced as a scenario for the MINLP (Eq. 18). This generates a new mechanism that is checked for flexibility by solving Eq. 20, and this procedure is iterated until $\chi \leq \epsilon$.

Obviously, this formulation is computationally more intensive than the mechanism reduction at nominal conditions. The numerical difficulties one typically encounters while trying to solve the problem as set up here arise mainly from the nonconvex nature of the problem, that implies the requirement of multiple initial points in order to ensure optimality of the solution of the flexibility problem (Eq. 20). Further discussion regarding the solution of both problems (Eqs. 18 and 20) can be found in Halemane and Grossmann (1983), Androulakis (2000), and Sirdeshpande et al. (2001). It should be noted that the number of iterations of the complete procedure (and, hence, computational time) is directly related to how close the initial set of reactions considered is to a set of reactions that constitute a final solution of the problem.

Owing to the coupled nature of uncertainty and sensitivity analyzes, the approach taken in this work was to efficiently and accurately capture the uncertainty characteristics of the system using SRSM and then to extract sensitivity information which would be useful in reducing the computational burden associated with the solution of the multiperiod optimization problem. This is accomplished by fixing the values of some of the variables based on SRSM approximated sensitivity and carrying out the Branch & Bound analysis on the remaining set via a procedure defined in a later section of this paper (Proposed framework for mechanism reduction). The Branch & Bound problem solved is, thus, of a greatly reduced size and requires comparatively much fewer number of nodes resulting in significantly less computational time.

Sensitivity Analysis Using SRSM

If uncertainty characteristics of the system under investigation are well captured by an SRSM expansion of appropriate order, uncertain model output concentrations at chosen points in time y_t can be well expressed as polynomial chaos approximations U_1, U_2, and U_3, as described in Eqs. 3, 4 and 5.

In order to obtain sensitivity information (the extent of change of an output with respect to a corresponding change in an input) from the outputs as approximated by an SRSM expansion, they are first differentiated with respect to each input srv. This gives (for a second-order SRSM approximation)

$$\frac{dy_{l,t,2}}{d\xi_i} = a_{l,t,i,2} + 2a_{l,t,ii,2}\,\xi_i + \sum_{j=1, j\neq i}^{n} a_{l,t,ij,2}\,\xi_j \tag{22}$$

using the fact that the srv's are independent.

The other required component in the derivation of sensitivity from the SRSM expansion is the exact parametric representation of uncertainty. In this work, all the uncertainty is considered in the rate constant values (which are expressed in modified Arrhenius form), and are also transformed solely to preexponential factor uncertainty. In the literature values of uncertainty factors in the rate constant, values were assumed to hold at the reaction temperatures considered, and based on these values, corresponding preexponential factor uncertainty parameters were subsequently calculated. The distributions of the preexponential factors, and consequently reaction rate constants, were chosen to be log-normal, which is a common parameterization for reaction rate constants, mainly due to the desirable attribute of nonnegativity. Transformation of these log-normal random variables to srv's (Table 1) yields

$$\begin{aligned} k_{f,i,t} &= A_i(\xi)e^{-E_i/(RT_t(\xi))}T_t(\xi)^{b_i} \\ &= e^{(\mu_i+\sigma_i\xi)}e^{-E_i/(RT_t(\xi))}T_t(\xi)^{b_i} \end{aligned} \tag{23}$$

where the parameters are obtained as $\mu_i = \log(A_i^{\text{nom}})$ and $\sigma_i = \log(UF_i)/2$, where A_i^{nom} is the nominal value of the preexponential factor of the ith reaction and the calculation of σ_i relies on the assumption that approximately 95% confidence intervals $(\pm 2\sigma_i)$ on the log-normal random variables correspond to the upper and lower bound as defined by the uncertainty factors (UF_i) of the reaction rate constant values. The temperature of the reaction $T_t(\xi)$ may or may not be constant depending on the process conditions considered. This leads to the derivation of normalized sensitivity for two distinct cases, namely, isothermal and nonisothermal conditions.

- For isothermal process conditions ($T_t(\xi) = T_0$ and $k_{f,i,t} = k_{f,i}$), we have

$$\frac{dk_{f,i}}{d\xi_i} = \sigma_i k_{f,i} \tag{24}$$

The normalized sensitivity of an output species l with respect to reaction i (at time t based on a second-order SRSM approximation), $\psi_{l,i,t,2}$, can be evaluated by the application of the chain rule

$$\psi_{l,i,t,2} = k_{f,i}\frac{dy_{l,t,2}}{dk_{f,i}} = k_{f,i}\left(\frac{dy_{l,t,2}}{d\xi_i}\right)\left(\frac{d\xi_i}{dk_{f,i}}\right) \tag{25}$$

which, combining Eqs. 22 and 24, yields the final simplified expression for the normalized sensitivity as

$$\psi_{l,i,t,2} = \frac{a_{l,t,i,2}}{\sigma_i} + \frac{2a_{l,t,ii,2}\,\xi_i}{\sigma_i} + \frac{\sum_{j=1,j\neq i}^{n} a_{l,t,ij,2}\,\xi_j}{\sigma_i} \tag{26}$$

- For nonisothermal process conditions, temperature is just another model output akin to the species concentration profiles. An SRSM expansion of the appropriate order can then be fit to the temperature profile at each point in time as well. For example, shown below is the temperature in the reactor modeled as a second-order SRSM expansion

$$T_{t,2}(\xi) = a_{T,t,0,2} + \sum_{i=1}^{n} a_{T,t,i,2}\,\xi_i + \sum_{i=1}^{n} a_{T,t,ii,2}(\xi_i^2 - 1) + \sum_{i=1}^{n-1}\sum_{j>i}^{n} a_{T,t,ij,2}\,\xi_i\xi_j \tag{27}$$

The normalized sensitivity, $\psi_{l,i,t,2}$, is found, in this case, to be

$$\psi_{l,i,t,2} = \frac{a_{l,t,i,2} + 2a_{l,t,ii,2}\,\xi_i + \sum_{j=1,j\neq i}^{n} a_{l,t,ij,2}\,\xi_j}{\sigma_i + \dfrac{b}{T_t(\xi)}\dfrac{dT_t(\xi)}{d\xi} + \dfrac{E}{RT_t(\xi)^2}\dfrac{dT_t(\xi)}{d\xi}} \tag{28}$$

It is worth pointing out here that, assuming the uncertainty characteristics of the system under consideration are well represented by an SRSM expansion, application of the preceding procedure results in a functional form (given by Eqs. 26 and 28) that enables computationally an inexpensive evaluation of the dependency of normalized sensitivity of a given reaction species l, with respect to a given reaction rate constant value $k_{f,i,t}$, at a chosen point in time t that is valid over the range of the uncertain rate constant values.

Proposed Framework for Mechanism Reduction

Following the scheme outlined in the previous section, the SRSM polynomial expansion coefficients can be used to extract sensitivity information from the reaction mechanism at different points in time while taking uncertainty into account. Sensitivity information is typically employed in kinetic mechanism reduction, as it provides a direct measure of the effect of change in the rate constant value on the output species of interest. Consequently, given the sensitivity information for a target output species, one effectively identifies which reactions dominate its profile at a given point in time.

In order to generate good initial sets of fixed reactions for both mechanism reduction optimization problems, the approach adopted in this work was to consider a threshold value for weight factors (derived from the ratio of the magnitude of the normalized sensitivities) as the criteria for judging which reactions are critical to the development of its profile. Any reactions whose weight factors exceed this threshold at any point of time and for any species were kept, and the remaining less important reactions were eliminated.

This methodology allows for an intuitive heuristic algorithm for generation of the initial set of reactions based on the relative magnitude of the normalized sensitivity of each reaction on the output species of interest. The details of the algorithm are as follows:

(1) Set $\boldsymbol{\xi} = \mathbf{0}$ (for reduction at nominal conditions) or find $\boldsymbol{\xi}$ such that $\boldsymbol{\xi} = \arg\max\,(\psi_{l,i,t})_{\boldsymbol{\xi}}$ (for reduction considering uncertainty). Note that the second problem is just a linear program in the case of isothermal conditions and a nonlinear optimization problem in the case of nonisothermal conditions.

(2) Select a threshold value δ.

(3) Compute the values of all the relative weights, $\omega_{l,i,t}$ (that is, for all reactions in the full mechanism), for a chosen output species by evaluating the percentage ratio of the absolute values of the normalized sensitivity, that is, $\omega_{l,i,t} = |\psi_{l,i,t}|/(\sum_{i=1}^{n}|\psi_{l,i,t}|) * 100$.

(4) Reject reactions whose relative weights are less than the chosen tolerance, that is, for a species l at time t, reject reaction i if $\omega_{l,i,t} < \delta$.

(5) Loop this procedure over all time points, t, and species of interest, l, with the final set of reactions equaling the union of all the reactions that satisfy the tolerance criterion, that is, the union of the reactions that are not rejected over all species and points in time.

Equations 26 and 28 provide the means of determining normalized sensitivity over the entire range of inputs (provided that the SRSM expansion is a good approximation to the system characteristics). The nominal response corresponds directly to setting $\boldsymbol{\xi} = \mathbf{0}$. When considering uncertainty and the task of providing the initial set for the multiperiod optimization problem, the set of $\boldsymbol{\xi}$ is determined such that the sensitivity of the ith reaction is maximum. At this value of $\boldsymbol{\xi}$ the relative weight of reaction i, $\omega_{l,i,t}$, is evaluated and compared to the tolerance value, δ. The selection of $\boldsymbol{\xi}$ following this approach fully exploits the fact that the SRSM framework obtains sensitivity information while taking uncertainty into account. In this manner, only reactions that are truly ineffectual over the whole reaction time interval, in terms of normalized sensitivity and with respect to the user-specified tolerance δ, are eliminated.

Two reaction systems have been studied in this article to illustrate the application of SRSM to uncertainty analysis of complex kinetic models. The remainder of this article describes the application of these ideas to these mechanisms, the first being a supercritical wet oxidation process, followed by a H_2/CO/air combustion mechanism.

Case Study A: SCWO

The subject of the first case study is a supercritical wet oxidation (SCWO) process, the details of which can be found in (Phenix et al., 1998), and is essentially a high-pressure (246 bar) oxidation of hydrogen and oxygen. The temperature of the process was assumed to remain constant at 823 K (used to determine the reaction rates) and the time of reaction considered was 10 s. Each forward rate constant corresponds to a random variable following a log-normal probability distribution, with the known median value and multiplicative uncertainty factor taken from the literature (Phenix et al., 1998; Tsang and Hampson, 1986; Atkinson et al., 1989; Baulch et al., 1992) and assumed to hold at the reaction temperature considered. Species thermochemical data were taken from the CHEMKIN database (Kee et al., 1996). The isothermal, tubular reactor modeled in this study was assumed to be well approximated by the plug-flow idealization, resulting in the governing species conservations equations reducing to a set of coupled, nonlinear, first-order, ordinary differential equations. These were solved using the deterministic stiff ODE solver, LSODE (Hindmarsh, 1983), and the details of the full mechanism itself can be found in Appendix A.

For mechanism reduction (both at nominal conditions and considering uncertainty), the following species profiles were tagged: H_2, O_2, HO_2, and H_2O. Thus, the objective of the optimization problems was to match the profiles of these species using a reduced mechanism while staying within a tolerance level ϵ.

Application of SRSM

Initial reaction rate constant uncertainty results in each reaction output (species concentration, temperature profile, and so on), becoming a stochastic process (a collection of profiles rather than a single profile), with time-varying distributions. The first step in the analysis was to apply SRSM of the appropriate order to the tagged output species at different time points in order to capture this time-varying nature of the distributions. Thus, at discrete points in time (between the reaction start and completion times) for each output species whose profile was to be matched for the mechanism reduction problem, an SRSM expansion was evaluated.

For the present isothermal mechanism case study, the total system reaction time was divided into ten equal time intervals between the time of reaction initiation ($t_0 = 0$) and reaction completion ($t_f = 10$ s), and SRSM polynomials were fit to each of the matched species' profiles (H_2, O_2, HO_2, and H_2O) at each of these points in time (at intervals of every second).

Once the SRSM analysis was complete (all the relevant coefficients determined for the output species at relevant time points), threshold values of δ were chosen and the algorithm as outlined in the previous section applied to both nominal and reduction under uncertainty cases to generate initial sets of reactions for the optimization problems.

Results

It was verified that the uncertainty in the predicted species concentration profiles varies with time, as shown previously by Phenix et al. (1998). Since the initial mole fractions were taken to be deterministic quantities, the uncertainty in predicted species concentrations arose solely due to the uncertainty in the initial reaction rate coefficients. Monte Carlo simulation was carried out involving random instantiations from the given distributions (15,000 model simulations) as a comparative method to analyze the uncertainty propagation characteristics of the system.

In addition, first- and second-order SRSM were used to predict the responses for the SCWO model requiring only 39 and 723 model simulations, respectively. Second-order SRSM expansions were found to be sufficient for this case study, and the close similarity of the probability distributions obtained at various points in time show the accuracy and efficiency of SRSM at capturing the uncertainty characteristics of this system. The choice of order of polynomial expansion was further ratified by error analysis. The mean squared er-

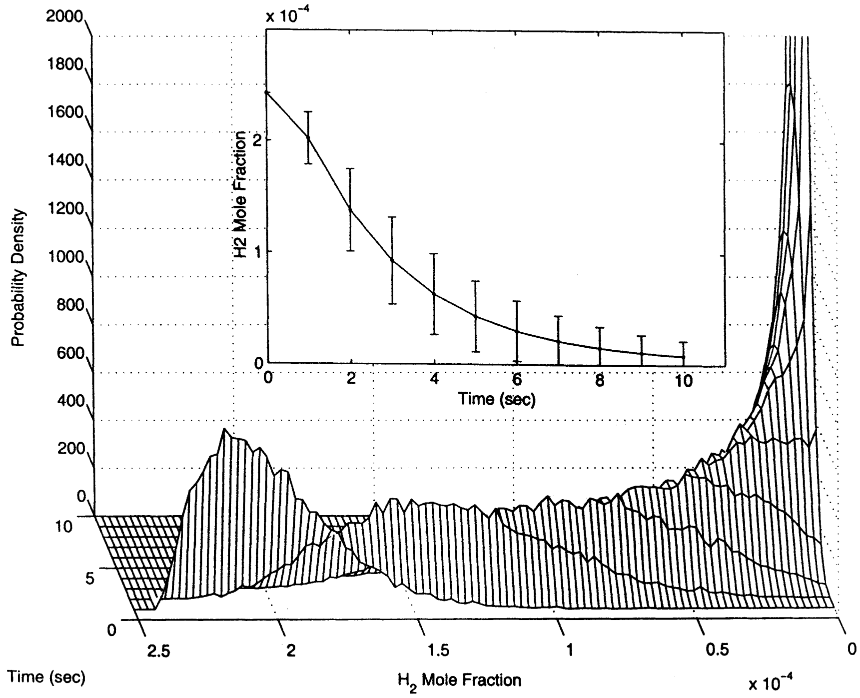

Figure 2. Time-evolving profile of the H_2 mole fraction for the SCWO system.

The inset (top center) shows the mean H_2 mole fraction evolution in time, with bars (above and below) illustrating the value of the standard deviation of the density function at the particular instant in time.

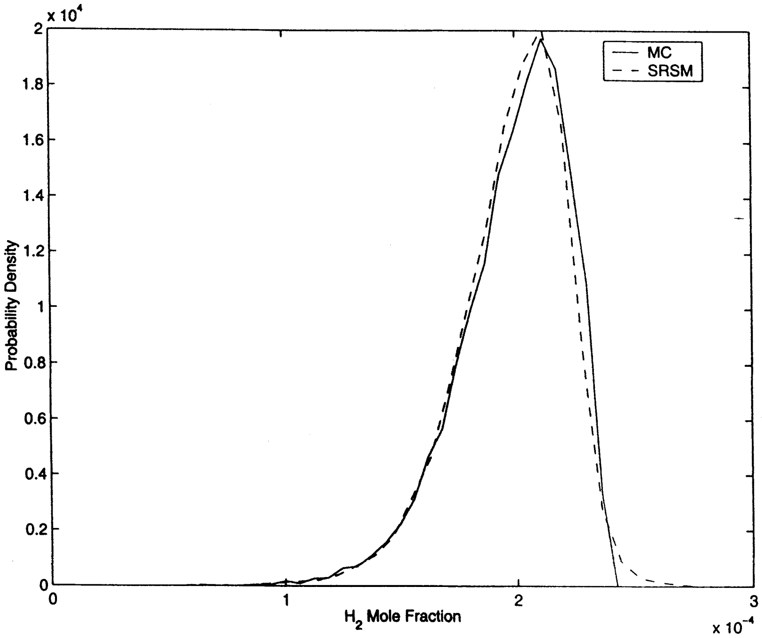

Figure 3. Probability densities of the H_2 mole fraction at $t = 1$ s (SCWO system): Monte Carlo vs. SRSM.

ror estimates $\widehat{MSE}$, defined as $\widehat{MSE} = (1/N)\,\Sigma_{i=1}^{N}(y^f - y^{srsm})^2$ (where y^f and y^{srsm} are the outputs of the full model and SRSM polynomial approximation, respectively, and N is the number of points at which these values are evaluated—in this case, the 15,000 random points used for the Monte Carlo simulation) were found to vary in magnitude between 8.8×10^{-12} (at $t = 1$ s) and 1.4×10^{-11} (at $t = 10$ s) for H_2 (which is representative of the other system species as well) and deemed suitable for the case study.

The uncertainty in each species mole fraction was found to increase until it reached a maxima (near $t = 2$ s) and then dropped to zero due to the fact that almost any combination of reaction rate constants predicts the completion of the reactions at large residence times. Figure 2 shows the time-evolving profiles (for the MC simulations of the full model) of H_2. The distribution at time $t = 0$ is just a delta function (owing to the initial concentration being a deterministic quantity) and not included in the plot.

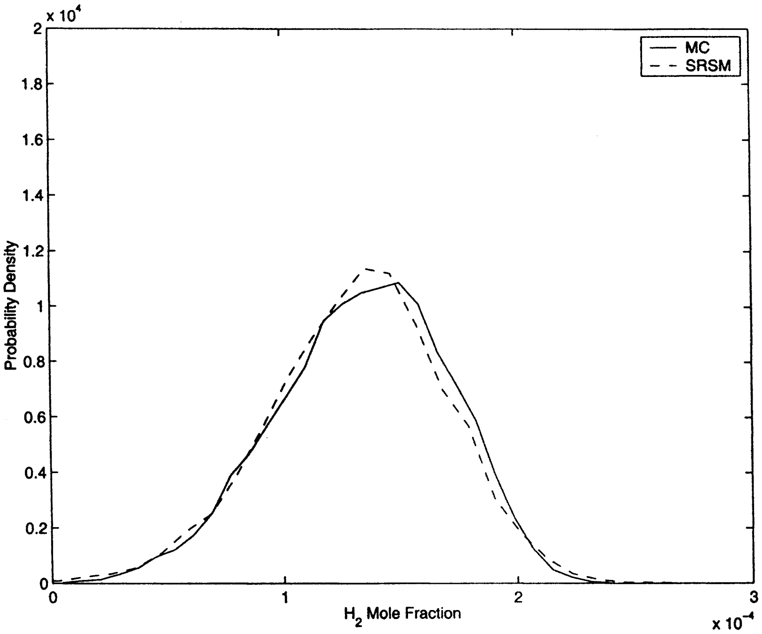

Figure 4. Probability densities of the H_2 mole fraction at $t = 2$ s (SCWO system): Monte Carlo vs. SRSM.

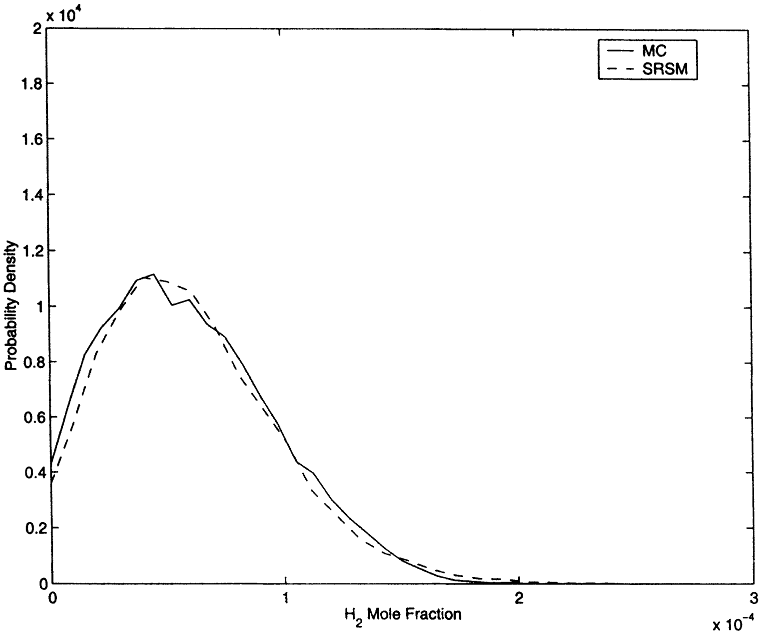

Figure 5. Probability densities of the H_2 mole fraction at $t = 4$ s (SCWO system): Monte Carlo vs. SRSM.

Figures 3, 4, and 5 indicate that the probability densities of the species of interest are very well represented by second-order SRSM expansions (by comparison to those generated by the Monte Carlo simulation of the problem). Shown are the densities of H_2 at $t = 1$, 2, and 4 s.

We subsequently attempted to verify that the sensitivity information obtained through SRSM expansion coefficients was also accurate. A comparison of the weights ($\omega_{l,i,t}$) as obtained through normalized sensitivity values determined using SRSM was made to those obtained from SENKIN (Lutz et al., 1990; which is a commercial package that can evaluate sensitivity in homogeneous gas-phase chemical kinetic systems). SENKIN displays normalized sensitivity coefficients with respect to reaction rates defined by

$$\varphi_{i,l,t} = \frac{k_i}{\max\{y_{i,l}\}} \frac{dy_{i,t}}{dk_i} \tag{29}$$

The $\psi_{l,i}$ obtained from the SRSM expansion coefficients had to be scaled by $\max\{y_{i,l}\}$ to reflect comparable quantities. The weights $\omega_{l,i,t}$ were then computed for the nominal values of reaction rate constants from both SRSM as well as SENKIN, and these are shown in Tables 2 and 3. The close similarity of the weights obtained from both methods verifies that the information obtained using the coefficients of SRSM expansions is indeed very representative of the sensitivity.

Table 2. Weight Values ($\omega_{H_2,i,t}$) from SENKIN at Various Time Points for H_2 (SCWO System)

	Time (s)				
Reaction	2.02	4.18	6.04	8.08	10.0
1	0.0007	0.0015	0.0023	0.0035	0.0048
2	24.8307	31.6615	32.4194	31.5528	30.0512
3	0.5235	1.0886	1.8324	3.1842	4.8333
4	10.655	8.2465	6.9772	5.8474	4.9583
5	25.2013	21.5008	21.8479	22.8975	23.9573
6	1.7696	1.2066	0.8965	0.6774	0.5401
7	23.6262	17.7812	15.0821	12.8527	11.1721
8	13.1565	18.3256	20.7202	22.7527	24.256
9	0.0525	0.05	0.044	0.0376	0.0328
10	0.0001	0.0001	0	0	0
11	0.0002	0.0002	0.0001	0.0001	0.0001
12	0	0	0	0	0
13	0.0233	0.0249	0.0279	0.033	0.0381
14	0.1047	0.0462	0.0889	0.1091	0.1117
15	0.0002	0.0002	0.0002	0.0001	0.0001
16	0.0556	0.0663	0.0609	0.0518	0.0437
17	0	0	0	0	0
18	0	0	0	0	0
19	0	0	0	0	0

Table 3. Weight Values ($\omega_{H_2,i,t}$) from SRSM Expansion Coefficients at Various Time Points for H_2 (SCWO System)

	Time (s)				
Reaction	2.0	4.0	6.0	8.0	10.0
1	0.0205	0.0372	0.0558	0.0774	0.1008
2	24.6541	30.3269	30.5451	29.612	28.3336
3	1.2053	2.13	3.2652	4.8553	7.0342
4	10.7382	8.3374	6.8162	5.5222	4.4566
5	25.6403	21.6041	21.3665	21.422	21.5453
6	1.8737	1.2983	0.9359	0.6883	0.5263
7	22.5722	18.1556	16.401	15.1528	13.4781
8	13.0393	17.8513	20.3132	22.3557	24.2016
9	0.0684	0.0659	0.0596	0.0547	0.0526
10	0.0001	0.0001	0.0001	0	0
11	0.0005	0.0005	0.0004	0.0003	0.0002
12	0.0001	0.0001	0	0	0
13	0.0322	0.0348	0.0399	0.047	0.0566
14	0.0839	0.0737	0.1237	0.1443	0.1535
15	0.0003	0.0003	0.0002	0.0002	0.0002
16	0.0698	0.0826	0.076	0.0667	0.059
17	0.0012	0.0013	0.0012	0.0012	0.0012
18	0	0	0	0	0
19	0	0	0	0	0

Table 4. Initial Reaction Sets for SCWO by SRSM-Based Sensitivity Analysis and Final Optimal Reduced Mechanisms (with Different Tolerance Values) for Reduction at Nominal Conditions

δ	Initial Reaction Set*	ϵ	Final Reaction Set**
5.0	2, 4, 5, 7, 8	0.1	2–8
0.5	2–8, 14	0.01	2–8, 13, 14, 16
0.1	2–8, 14	0.001	2–10, 13–16

*Provided by proposed SRSM framework.
**Obtained via solution of optimization problem.

Table 5. Initial Reaction Sets for SCWO by SRSM-Based Sensitivity Analysis and Final Optimal Reduced Mechanisms (with Varying Tolerance Values) for Reduction Considering Uncertainty

δ	Initial Reaction Set	ϵ	Final Reaction Set
5.0	2–8, 14	0.1	2–8, 13, 14, 16
0.5	2–10, 13–16	0.01	1–10, 13–16
0.1	2–11, 13–16	0.001	Whole set (1–19)

Note: The final (optimal) mechanisms shown here are obtained by application of Multiperiod analysis.

Finally, initial sets of reactions were generated for different threshold values and both mechanism reduction optimization problems solved using these initial sets. The results are detailed in Tables 4 and 5. As can be observed, the initial sets generated are very close in both cases to the actual final reduced mechanisms obtained after the complete solution of both the multiperiod and nominal reduction problems. This, of course, involves the judicious choice of tolerance values (both for the initial sets δ and final optimization problems ϵ), which are, by definition, user-specified parameters. The choice of tolerance naturally depends on a variety of factors, including number and choice of species whose profiles are being matched and a degree of closeness to original profiles is considered acceptable, and, thus, cannot be specified in a general manner.

Table 6. SRSM Framework vs. Existing Pseudosensitivity-Based Framework for SCWO Considering Reduction under Uncertainty

	Pseudosensitivity		SRSM Framework	
	δ		ϵ	
No. of scenarios	0.1	3	5.0	2
	0.01	3	0.5	1
	0.001	1	0.1	1
Total CPU time (s)	0.1	391.6	5.0	580.1
	0.01	560.2	0.5	152.3
	0.001	405.83	0.1	72.78
Final reaction set	0.1	2–8, 13, 14, 16	5.0	Same
	0.01	1–10, 13–16	0.5	Same
	0.001	Whole set (1–19)	0.1	Same

Table 6 also shows the comparison between the proposed SRSM framework and the existing pseudosensitivity-based framework for reduction of the SCWO mechanism under uncertainty conditioned on various values of the tolerance (ϵ = 0.1, 0.01, and 0.001). As can be seen, the number of scenarios is reduced (as predicted), and the CPU times reflect significant savings in computational time (the one exception being the high tolerance $\delta = 0.1$ case where the pseudosensitivity directly gives the solution).

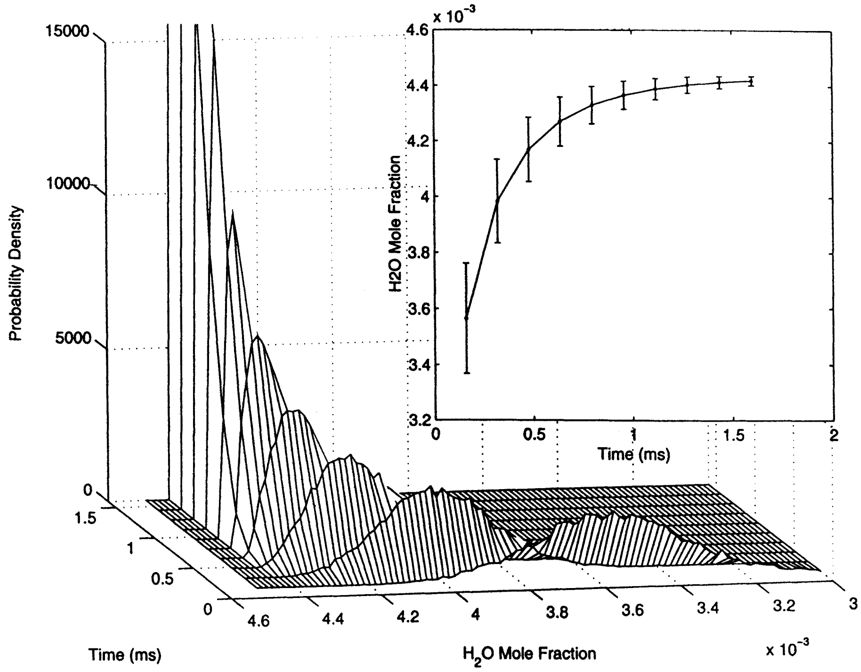

Figure 6. Time-evolving probability densities of H_2O mole fraction for the H_2/CO/air mechanism.

The inset (top right) shows the mean H_2O mole fraction evolution in time with bars (above and below) illustrating the value of the standard deviation of the density function at the particular instant in time. The H_2O mole fraction at $t = 0$ has been omitted for clarity.

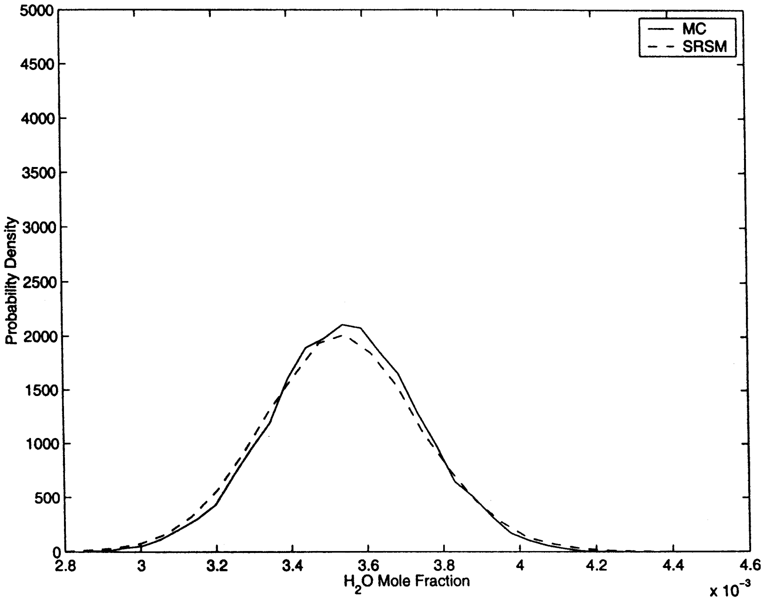

Figure 7. Probability densities of H_2O at $t = 0.16$ ms (H_2/CO/air system): Monte Carlo (MC) vs. SRSM.

Case Study B: H_2/CO/Air Mechanism

The second system investigated models the combustion of a syngas mixture in air (Androulakis, 2000), details in (Li and Rabitz, 1997), and contains 47 reversible reactions and 13 species (see Appendix B for mechanism details). Initial process conditions were taken to be deterministic ($x_{H_2} = 0.005$, $x_{O_2} = 0.189$, $x_{CO} = 0.095$, $x_{N_2} = 0.711$, and $T_0 = 1600$ K), with uncertainty incorporated into the rate coefficients as in the previous case study by modeling the uncertainty as existing purely in the preexponential factors of the rate constant expressions with log-normal distributions. For the purposes of this exploratory case study, all the uncertainty factors were taken to be equal to 3.333, merely to facilitate the understanding of uncertainty propagation in the system and observe representative effects on mechanism reduction.

The specifications for both mechanism-reduction problems (considering uncertainty and at nominal conditions) was to match the profiles of the following outputs: H_2, O_2, H_2O, CO, CO_2, and T within ϵ tolerance.

Application of SRSM

The SRSM analysis applied to this case study was very similar to that employed in the SCWO process, with the notable difference of the process conditions being nonisothermal. Also, temperature being one of the tagged species required it

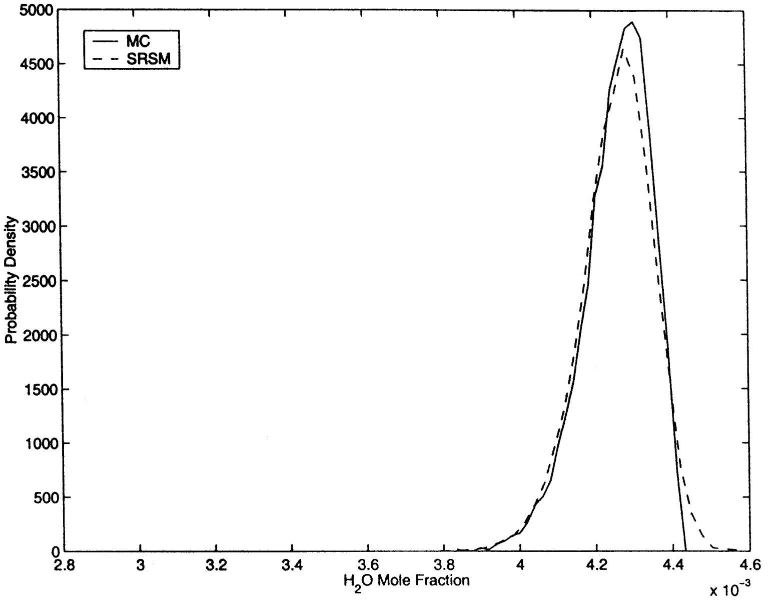

Figure 8. Probability densities of H_2O at $t = 0.64$ ms (H_2/CO/air system): Monte Carlo (MC) vs. SRSM.

Table 7. Initial Reaction Sets for H_2/CO/Air by SRSM-Based Sensitivity Analysis and Final Optimal Reduced Mechanisms for Reduction at Nominal Conditions and Reduction Considering Uncertainty

Case	Initial Reaction Set	Final Reaction Set
Nominal reduction	1, 4, 6, 10, 12–15, 17, 22, 25, 35, 37, 38, 43	1–4, 6, 10, 12–15, 17, 22, 24, 25, 32–35, 37, 38, 43
Reduction considering uncertainty	1–6, 10, 12, 13–15, 17, 18, 22–26, 33–38, 42, 43, 46, 47 S $\delta = 2.5$; $\epsilon = 0.001$	1–7, 10, 12–15, 17, 18, 22–26, 32–38, 42, 43, 46, 47

to be approximated via an SRSM expansion in a manner similar to any reaction species (Eq. 27).

In this case, too, the presence of uncertainty in the reaction rate constants resulted in time-varying distributions for process outputs. The total system reaction time was also divided into ten equal time intervals between the time of reaction initiation ($t_0 = 0$) and reaction completion ($t_f = 1.6$ ms), and SRSM polynomials were fit to each of the matched species' profiles (including temperature) at each of these discrete points in time.

Once the SRSM analysis was completed (with all the relevant coefficients determined for the output species at a relevant time point), a threshold δ was chosen and initial sets of reactions for both of the optimization problems were generated.

Results

The time-varying nature of the distributions of species profiles (such as Figure 6 for H_2O) at each point in time were captured well by second-order SRSM expansions in this case as well (Figures 7 and 8). This can clearly be seen by the comparison of distributions obtained to those from a Monte Carlo analysis of the system performed, which required 15,000 model simulations (plots are at $t = 0.16$ and 0.64 ms into the reaction for H_2O). In contrast, second-order SRSM required only 4419 simulations. The choice of order of expansion was further ratified by the $\widehat{MSE}$ estimates obtained (once again from the 15,000 points used in the Monte Carlo analysis) for H_2O (representative species for this system), which ranged in magnitude from 2.5×10^{-11} (at $t = 1.28$ ms) to 9.4×10^{-7} (at $t = 1.6$ ms).

The values of the initial reaction sets generated using the SRSM framework are shown in Table 7 along with the final mechanism obtained by the solution of the optimization problems (nominal mechanism reduction and the multiperiod formulation, that is, reduction under uncertainty). The table shows that the initial sets generated are very close in both cases to the actual final reduced mechanisms obtained after the complete solution of the integer programming problem. Once again, Table 8 highlights the reduction in the number of scenarios and the significant savings in computational time achieved by the application of the proposed SRSM framework as compared to the existing pseudosensitivity-based framework of analysis when considering a reduction under reaction rate constant uncertainty.

Table 8. SRSM Framework vs. Existing Pseudosensitivity-Based Framework for H_2/CO/Air Considering Reduction Under Uncertainty

	Pseudosensitivity $\delta = 0.001$	SRSM Framework $\epsilon = 2.5$
No. of scenarios	6	3
Total CPU time (s)	42,814.9	15,900.8
Final reaction set	1–8, 10, 12, 13–15, 17, 18, 22–26, 32–38, 43, 46, 47	1–7, 10, 12, 13–15, 17, 18, 22–26, 32–38, 42, 43, 46, 47

Conclusions and Future Directions

This article focused on the problem of taking into account uncertainty effects of reaction rate constant values when dealing with complex kinetic reaction mechanisms. SRSM, an efficient and accurate uncertainty analysis technique, proved extremely useful in the systematic characterization of uncertainty. A novel computationally efficient framework of analysis was outlined, by which good initial sets of variables for the reaction mechanism reduction (both at nominal conditions and considering uncertainty) can be generated and correspondingly computationally smaller optimization problems solved. In addition, the analysis using SRSM was found to provide a straightforward and efficient method of determining the sensitivity of reaction-mechanism species with respect to reaction rates, taking uncertainty into account.

Many extensions to this work could be envisioned, including taking various other distributions for the rate constants into account (this work only considers log-normal distributions), as well as utilizing the coefficients obtained from SRSM expansions, to provide valuable insight into the dynamics of the reaction mechanism itself. Also, the framework lends itself to extension in the form of parameterizing all factors of uncertainty independently (uncertainties in activation energy values, temperature exponents, and so on) that would result in a systematic method of analysis that could take into account all possible sources of uncertainty in reaction rate constants.

Overall, an accurate, systematic, and efficient framework of analysis has been detailed, which eases the computational burden associated with the complex reaction mechanism reduction as well as aids the understanding of the uncertainty effects in such systems.

Acknowledgments

The authors gratefully acknowledge support from the USEPA funded Center for Exposure and Risk Modeling (CERM) under Cooperative Agreement # EPAR-827033, the NJDEP funded Ozone Research Center (ORC), the NSF Career Award (CTS division No. 998306), and the donors of the Petroleum Research Fund (administered by the ACS).

Literature Cited

Androulakis, I. P., "Kinetic Mechanism Reduction Based on an Integer Programming Approach," *AIChE J.*, **46**, 361 (2000).

Atkinson, R., D. Baulch, R. Cox, R. Hampson, J. Kerr, and J. Troe, "Evaluated Kinetic and Photochemical Data for Atmospheric Chemistry," *J. Phys. Chem. Ref. Data*, **18**, 1127 (1989).

Baulch, D., C. Cobos, R. Cox, C. Esser, P. Frank, T. Just, J. Kerr, M. Pilling, J. Troe, R. Walker, and J. Warnatz, "Evaluated Kinetic Data for Combustion Modeling," *J. Phys. Chem. Ref. Data*, **21**, 411 (1992).

Ghanem, R., and P. Spanos, *Stochastic Finite Elements: A Spectral Approach*, Springer-Verlag, New York (1991).

Halemane, K., and I. Grossmann, "Optimal Process Design Under Uncertainty," *AIChE J.*, **29**, 425 (1983).

Hindmarsh, A. C., "Odepack, a Systematized Collection of ODE Solvers," *Numer. Methods Sci. Comput.*, **55** (1983).

Isukapalli, S. S., *Uncertainty Analysis of Transport-Transformation Models*, PhD Thesis, Rutgers Univ. (1999).

Isukapalli, S. S., A. Roy, and P. Georgopoulos, "Stochastic Response Surface Methods (SRSMs) for Uncertainty Propagation: Application to Environmental and Biological Systems," *Risk Anal.*, **18**(3), 351 (1998).

Isukapalli, S. S., A. Roy, and P. Georgopoulos, "Efficient Sensitivity/Uncertainty Analysis Using the Combined Stochastic Response Surface Method and Automated Differentiation: Application to Environmental and Biological Systems," *Risk Anal.*, **20**(5), 591 (2000).

Kee, R., F. Rupley, E. Meeks, and J. Miller, "Chemkin-III: A Fortran Chemical Kinetics Package for the Analysis of Gas-Phase Chemical and Plasma Kinetics," Tech. Rep., Environmental Quality Laboratory, California Institute of Technology, Sandia Report m SAND96-8216 (1996).

Li, G., and H. Rabitz, "Reduced Kinetic Equations of a CO/H$_2$/Air Oxidation Model by a Special Perturbation Method," *Chem. Eng. Sci.*, **52**, 4317 (1997).

Lutz, A., R. Kee, and J. A. Miller, "Senkin: A Fortran Program for Predicting Homogeneous Gas Phase Chemical Kinetics With Sensitivity Analysis," Tech. Rep., Sandia National Laboratories, Albuquerque, NM (1990).

Phenix, B. D., J. L. Dinaro, M. A. Tatang, W. A. Tester, J. B. Howard, and G. J. McRae, "Incorporation of Parametric Uncertainty into Complex Kinetic Mechanisms: Application to Hydrogen Oxidation in Supercritical Water," *Combust. Flame*, **112**, 132 (1998).

Sirdeshpande, A. R., M. G. Ierapetritou, and I. P. Androulakis, "Design of Flexible Reduced Kinetic Mechanisms," *AIChE J.*, **47**, 2461 (2001).

Tatang, M. A., *Direct Incorporation of Uncertainty in Chemical and Environmental Engineering Systems*, PhD Thesis, Massachusetts Institute of Technology, Cambridge (1995).

Tsang, W., and R. Hampson, "Chemical Kinetic Data Base for Combustion Chemistry. Part I. Methane and Related Compounds," *J. Phys. Chem. Ref. Data*, **15**, 1087 (1986).

Villadsen, J., and M. Michelsen, *Solution of Differential Equation Models by Polynomial Approximation*, Prentice Hall, Englewood Cliffs, NJ (1978).

Appendix A: SCWO Mechanism Details

Table A1. Full SCWO Mechanism

		$k_{f,i} = A_i e^{-E_i/RT} T^{b_i}$			
	Reactions Considered	A_i	b_i	E_i/R	UF
1	$OH + H \rightarrow H_2O$	1.62×10^{14}	0.0	75.0	3.16
2	$H_2 + OH \rightarrow H_2O + H$	1.02×10^{8}	1.6	1,660.0	1.26
3	$H + O_2 \rightarrow HO_2$	1.48×10^{12}	0.6	0.0	1.58
4	$HO_2 + HO_2 \rightarrow H_2O_2 + O_2$	1.87×10^{12}	0.0	775.0	1.41
5	$H_2O_2 + OH \rightarrow H_2O + HO_2$	7.83×10^{12}	0.0	670.0	1.58
6	$H_2O_2 + H \rightarrow HO_2 + H_2$	1.69×10^{12}	0.0	1,890.0	2.00
7	$H_2O_2 \rightarrow OH + OH$	3.00×10^{14}	0.0	24,400.0	3.16
8	$OH + HO_2 \rightarrow H_2O + O_2$	2.89×10^{13}	0.0	−250.0	3.16
9	$H + O_2 \rightarrow OH + O$	1.99×10^{14}	0.0	8,460.0	1.16
10	$O + H_2 \rightarrow OH + H$	5.13×10^{4}	2.7	3,160.0	1.22
11	$2OH \rightarrow O + H_2O$	1.50×10^{9}	0.0	50.0	1.22
12	$H_2 + M \rightarrow H + H + M$	4.58×10^{19}	−1.4	48,350.0	3
13	$H + HO_2 \rightarrow OH + OH$	1.69×10^{14}	0.0	440.0	1.35
14	$H + HO_2 \rightarrow H_2 + O_2$	4.28×10^{13}	0.0	710.0	1.35
15	$O + HO_2 \rightarrow OH + O_2$	3.25×10^{13}	0.0	0.0	1.49
16	$H_2O_2 + H \rightarrow H_2O + OH$	1.02×10^{13}	0.0	1,800.0	1.35
17	$O + H + M \rightarrow OH + M$	4.71×10^{18}	−1.0	0.0	10
18	$O + O + M \rightarrow O_2 + M$	1.89×10^{13}	0.0	−900.0	1.3
19	$H_2O_2 + O \rightarrow OH + HO_2$	6.62×10^{11}	0.0	2,000.0	1.35

Units: E_i (K), A_i (mol·cm·s·K).

Appendix B: Full H_2/CO/Air Mechanism Details

Table B1. Full H_2/CO/Air Mechanism

		$k_{f,i} = A_i e^{(-E_i/RT)} T^{b_i}$		
	Reactions Considered	A_i	b_i	E_i/R
1	$2O + M \rightarrow O_2 + M$	1.20×10^{17}	−1.0	0.0
	H_2 Enhanced by 2.400			
	H_2O Enhanced by 1.540×10^{1}			
	CO Enhanced by 1.75			0
	CO_2 Enhanced by 3.600			
	AR Enhanced by 8.300×10^{-1}			
2	$O + H + M \rightarrow OH + M$	5.00×10^{17}	−1.0	0.0
	H_2 Enhanced by 2.000			
	H_2O Enhanced by 6.000			
	CO Enhanced by 1.500			
	CO_2 Enhanced by 2.00			0
	AR Enhanced by 7.000×10^{-1}			
3	$O + H_2 \rightarrow H + OH$	5.00×10^{4}	2.7	6,290.0
4	$O + HO_2 \rightarrow OH + O_2$	2.00×10^{13}	0.0	0.0
5	$O + H_2O_2 \rightarrow OH + HO_2$	9.63×10^{6}	2.0	4,000.0
6	$O + CO + M \rightarrow CO_2 + M$	6.02×10^{14}	0.0	3,000.0
	H_2 Enhanced by 2.000			
	O_2 Enhanced by 6.000			
	H_2O Enhanced by 6.000			
	CO Enhanced by 1.500			
	CO_2 Enhanced by 3.500			
	AR Enhanced by 5.000×10^{01}			
7	$O + HCO \rightarrow OH + CO$	3.00×10^{13}	0.0	0.0
8	$O + HCO \rightarrow H + CO_2$	3.00×10^{13}	0.0	0.0
9	$O + CH_2O \rightarrow OH + HCO$	3.90×10^{13}	0.0	3,540.0
10	$O_2 + CO \rightarrow O + CO_2$	2.50×10^{12}	0.0	47,800.0
11	$O_2 + CH_2O \rightarrow HO_2 + HCO$	1.00×10^{14}	0.0	40,000.0
12	$H + O_2 + M \rightarrow HO_2 + M$	2.80×10^{18}	−0.9	0.0
	O_2 Enhanced by 0.000			
	H_2O Enhanced by 0.000			
	CO Enhanced by 7.500×10^{1}			
	CO_2 Enhanced by 1.500			
	N_2 Enhanced by 0.000			
	AR Enhanced by 0.000			
13	$H + 2O_2 \rightarrow HO_2 + O_2$	3.00×10^{20}	−1.7	0.0
14	$H + O_2 + H_2O \rightarrow HO_2 + H_2O$	9.38×10^{18}	−0.8	0.0
15	$H + O_2 + N2 \rightarrow HO_2 + N2$	3.75×10^{20}	−1.7	0.0
16	$H + O_2 + AR \rightarrow HO_2 + AR$	7.00×10^{17}	−0.8	0.0
17	$H + O_2 \rightarrow O + OH$	8.30×10^{13}	0.0	14,413.0

Table B1. Full H_2/CO/Air Mechanism (continued)

		$k_{f,i} = A_i e^{(-E_i/RT)} T^{b_i}$		
	Reactions Considered	A_i	b_i	E_i/R
18	$2H + M \rightarrow H_2 + M$	1.00×10^{18}	−1.0	0.0
	H_2 Enhanced by 0.000			
	H_2O Enhanced by 0.000			
	CO_2 Enhanced by 0.000			
	AR Enhanced by 6.300×10^1			
19	$2H + H_2 \rightarrow 2H_2$	9.00×10^{16}	−0.6	0.0
20	$2H + H_2O \rightarrow H_2 + H_2O$	6.00×10^{19}	−1.2	0.0
21	$2H + CO_2 \rightarrow H_2 + CO_2$	5.50×10^{20}	−2.0	0.0
22	$H + OH + M \rightarrow H_2O + M$	2.20×10^{22}	−2.0	0.0
	H_2 Enhanced by 7.300×10^1			
	H_2O Enhanced by 3.650			
	AR Enhanced by 3.800×10^1			
23	$H + HO_2 \rightarrow O + H_2O$	3.97×10^{12}	0.0	671.0
24	$H + HO_2 \rightarrow O_2 + H_2$	2.80×10^{13}	0.0	1,068.0
25	$H + HO_2 \rightarrow 2OH$	1.34×10^{14}	0.0	635.0
26	$H + H_2O_2 \rightarrow HO_2 + H_2$	1.21×10^{7}	2.0	5,200.0
27	$H + H_2O_2 \rightarrow OH + H_2O$	1.00×10^{13}	0.0	3,600.0
28	$H + HCO(+M) \rightarrow CH_2O(+M)$	1.09×10^{12}	0.5	−260.0
	Low-pressure limit:			
	0.13500×10^{25} -0.25700×10^{01}			
	0.14250×10^{4}			
	TROE centering:			
	0.78240 0.27100×10^{3}			
	0.27550×10^{4}			
	0.65700×10^{4}			
	H_2 Enhanced by 2.000			
	H_2O Enhanced by 6.000			
	CO Enhanced by 1.500			
	CO_2 Enhanced by 2.000			
	AR Enhanced by 7.000×10^1			
29	$H + HCO \rightarrow H_2 + CO$	7.34×10^{13}	0.0	0.0
30	$H + CH_2O \rightarrow HCO + H_2$	2.30×10^{10}	1.1	3,275.0
31	$H_2 + CO(+M) \rightarrow CH_2O(+M)$	4.30×10^{7}	1.5	79,600.0
	Low-pressure limit:			
	0.50700×10^{28} -0.34200×10^{1}			
	0.84350×10^{5}			
	TROE centering:			
	0.93200 0.19700×10^{3}			
	0.15400×10^{4}			
	0.10300×10^{5}			
	H_2 Enhanced by 2.000			
	H_2O Enhanced by 6.000			
	CO Enhanced by 1.500			
	CO_2 Enhanced by 2.000			
	AR Enhanced by 7.000×10^1			
32	$OH + H_2 \rightarrow H + H_2O$	2.16×10^{8}	1.5	3,430.0
33	$2OH(+M) \rightarrow H_2O_2(+M)$	7.40×10^{13}	−0.4	0.0
	Low-pressure limit:			
	0.23000×10^{19} -0.90000			
	-0.17000×10^{4}			
	TROE centering:			
	0.73460 0.94000×10^{2}			
	0.17560×10^{4} 0.51820×10^{4}			
	H_2 Enhanced by 2.000			
	H_2O Enhanced by 6.000			
	CO Enhanced by 1.500			
	CO_2 Enhanced by 2.000			
	AR Enhanced by 7.000×10^1			
34	$2OH \rightarrow O + H_2O$	3.57×10^{4}	2.4	−2,110.0
35	$OH + HO_2 \rightarrow O_2 + H_2O$	2.90×10^{13}	0.0	−500.0
36	$OH + H_2O_2 \rightarrow HO_2 + H_2O$	1.75×10^{12}	0.0	320.0
37	$OH + H_2O_2 \rightarrow HO_2 + H_2O$	5.80×10^{14}	0.0	9,560.0
38	$OH + CO \rightarrow H + CO_2$	4.76×10^{7}	1.2	70.0
39	$OH + HCO \rightarrow H_2O + CO$	5.00×10^{13}	0.0	0.0
40	$OH + CH_2O \rightarrow HCO + H_2O$	3.43×10^{9}	1.2	−447.0
41	$2HO_2 \rightarrow O_2 + H_2O_2$	1.30×10^{11}	0.0	−1,630.0
42	$2HO_2 \rightarrow O_2 + H_2O_2$	4.20×10^{14}	0.0	12,000.0
43	$HO_2 + CO \rightarrow OH + CO_2$	1.50×10^{14}	0.0	23,600.0
44	$HO_2 + CH_2O \rightarrow HCO + H_2O_2$	1.00×10^{12}	0.0	8,000.0
45	$HCO + H_2O \rightarrow H + CO + H_2O$	2.24×10^{18}	−1.0	17,000.0
46	$HCO + M \rightarrow H + CO + M$	1.87×10^{17}	−1.0	17,000.0
	H_2 Enhanced by 2.000			
	H_2O Enhanced by 0.000			
	CO Enhanced by 1.500			
	CO_2 Enhanced by 2.000			
47	$HCO + O_2 \rightarrow HO_2 + CO$	7.60×10^{12}	0.0	400.0

Units: E_i (K), A_i (mol·cm·s·K).
Species X Enhanced by y refers to enhancement factor for third body reactions.
Please refer to CHEMKIN documentation (Kee et al., 1996) for details.

Manuscript received Jan. 22, 2002, and revision received July 10, 2002.